

Supplementary Material:

Lipid Rafts: Buffers of Cell Membrane Physical Properties

Jonathan D. Nickels^{1,*}, Micholas Dean Smith^{2,3}, Richard J. Alsop⁴, Sebastian Himbert⁴, Ahmad Yahya¹, Destini Cordner¹, Piotr Zolnierczuk⁵, Christopher B. Stanley⁶, John Katsaras^{6,7}, Xiaolin Cheng⁸, Maikel C. Rheinstädter⁴.

¹ Department of Chemical and Environmental Engineering, University of Cincinnati, Cincinnati, OH 45221; ²Center for Molecular Biophysics, Oak Ridge National Laboratory, Oak Ridge, TN 37830, USA; ³Department of Biochemistry and Cellular and Molecular Biology, University of Tennessee, Knoxville, TN 37996; ⁴Department of Physics and Astronomy, McMaster University, Hamilton, ON, L8S 4M1, Canada; ⁵Jülich Center for Neutron Science, Forschungszentrum Jülich GmbH, Outstation at SNS, Oak Ridge, TN 37830, USA; ⁶Large-scale structure group, Oak Ridge National Laboratory, Oak Ridge, TN 37830, USA; ⁷Shull-Wollen Center, Oak Ridge National Laboratory, Oak Ridge, TN 37830, USA; ⁸ College of Pharmacy, Medicinal Chemistry & Pharmacognosy Division, The Ohio State University, Columbus, OH 43210, USA.

This document contains supporting figures 1 and 2, supporting tables 1 and 2, and details describing the methodology and analysis of the MD simulations.

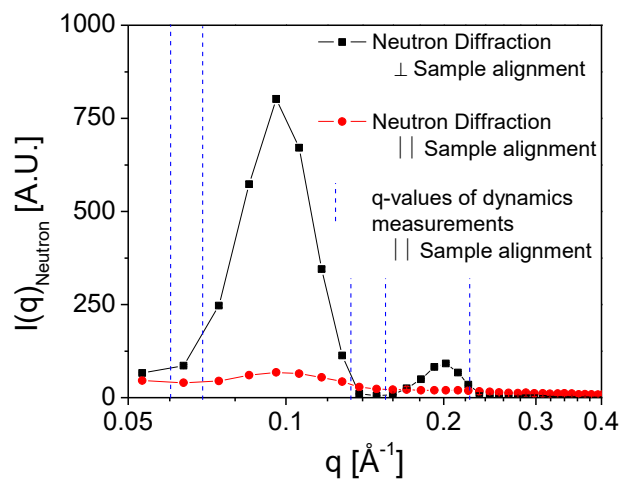


FIG. S1. The sample geometry was varied to align the scattering wave vector to parallel, \parallel , and perpendicular, \perp , with respect to the lipid bilayers. Diffraction measurements show the clear signatures of adjacent lamellae in the \perp configuration showing, which are substantially reduced in the \parallel configuration. The dashed vertical lines denote the q -values at which spin-echo measurements (NSE) were made in to avoid any influence from adjacent lamellae.

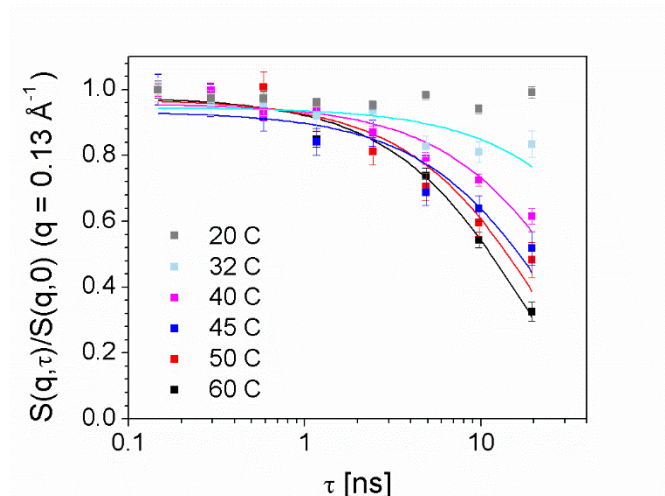


FIG. S2. Phase separation is apparent in the temperature dependence of structural relaxations in the aligned lipid bilayers. **(A)** Here we show the time scale of collective motions at fixed q ($q=0.13 \text{ \AA}^{-1}$) as a function of temperature for 0.45 mole fraction $d70$ -DSPC, $d70$ -DSPC/DMPC supported lipid bilayers in the II configuration. The solid lines are a single exponential fit to the data.

To complement the insights provided by the experimental results all-atom molecular dynamics simulations were performed for membranes consisting of entirely of DMPC and mixtures of DMPC with DSPC. SI Tables 1 and 2 summarize the simulation conditions and the simulation lengths. The membranes were constructed using the CHARMM-GUI¹⁻⁴ online interface with a total of 400 lipids (200 lipids per leaflet) and all simulations were performed using the GROMACS (2016.3) simulation package⁵.

Table S1. Summary of simulation length.

Single component DMPC	
Temp (°C)	Simulation Length
25	450ns
30	450ns
35	450ns
40	450ns
45	450ns
50	450ns
60	450ns

Table S2. Simulation box compositions and temperatures.

DSPC/DMPC mixtures		
Temp (°C)	c (mole fraction DSPC)	Simulation Length
25	0.15	950ns
38	0.28	550ns
40	0.36	550ns
45	0.45	550ns
50	0.45	550ns
55	0.45	550ns
60	0.45	550ns

The membrane structures generated from the CHARMM-GUI were subjected to a standard relaxation procedure: energy minimization and short restrained simulations with relaxing restraint strengths, as prescribed by the CHARMM-GUI developers. Briefly, for each system energy minimization (using the steepest decent method) was used until the threshold of 1000 kJ/mol/nm was reached, followed by six short restrained relaxation simulations. An integration timestep of 1 fs was used for the three relaxation simulations (each with a total simulation length of 25 ps), followed by a 2 fs timestep (and simulation lengths of 50 ps) for the remaining relaxation simulations. The first two relaxations were performed in the NVT ensemble using the Berendsen thermostat, while the remaining relaxation simulations were performed in a semi-isotropic (the z box dimension was uncoupled from the x and y box dimensions) using the Berendsen baro/thermostat⁶. For all relaxation simulations hydrogen positions were constrained with the LINCS algorithm⁷.

Single instance production simulations were then performed on the final relaxed structures using the Nose-Hoover thermostat⁸⁻¹⁰ (with a τ_t of 1ps) and Parrinello-Rahman barostat¹¹ (with a τ_p of 5ps), a 2fs integration timestep, frame saving rate (for analysis) of 10ps, and with hydrogen positions constrained using the LINCS algorithm.

Although relaxation of the initial membrane structure avoids unphysical clashes, the initial configurations are not guaranteed to be in a true equilibrium state and as such the simulations production simulations were carried out until the potential energy of the simulations no-longer exhibited a visible drift for at least 100ns. For the pure DMPC membranes this required no-more than 450ns of simulation time, while for the mixed systems (excluding the low temperature DMPC/DPSC mixture that is near a phase boundary), 550ns of simulation time was necessary.

Simulation Analysis

Analysis of the simulation was performed using a combination of internal GROMACS utilities, in-house VMD¹² scripts, and the SASSENA¹³ molecular dynamics neutron/X-ray analysis software package. For all analysis calculations performed the last 100ns of the simulations were used. From the simulations lateral diffusion constants, area per lipid, membrane thickness, bending moduli, and simulated neutron intermediate scattering functions (ISF) were obtained.

The lateral diffusion constants, area per lipid, and membrane thickness were calculated using the *gmx msd*, *gmx energy*, and *gmx density* utilities. For the diffusion constants, *gmx msd* computes the lateral (x/y) mean-squared displacement of the phosphate atoms from the lipid head-groups and performs a linear fitting to obtain the slope. Area per lipid is computed by calculating the product of the x/y box dimensions from the trajectory as a proxy for the membrane area and dividing by 200 (200 lipids per leaflet). The membrane thickness is estimated by computing the average transverse (membrane-normal) density profiles of the phosphate head-groups and taking the difference between the two maxima present (correlated with the two leaflets) as the average head-group/head-group distance.

The bending moduli for the systems were obtained using a VMD/tcl implementation of the calculations proposed by Khelashvili et al¹⁴. This method uses VMD to initially calculate the splay and tilt moduli of each individual lipid component, followed by

computing the splay between pairs of different lipid types, combining and reweighting these values to obtain the average bending modulus.

Compared to the size of the experimental system, the membrane simulated here is small. As a result, what would be considered minor-transverse fluctuations in experiment will produce large signals in ISF profiles calculated from the simulation. Hence, in order to allow comparison to the same dynamics examined by the neutron experiments, prior to the calculation of the ISF the z-direction motions of the lipids were removed using a combination of VMD (catdcd) and in-house awk scripts. Following this, the last 100ns of each of the reduced (z-removed) simulations were piped into the SASSENA software package.

References

1. Jo, S.; Kim, T.; Iyer, V. G.; Im, W., CHARMM-GUI: a web-based graphical user interface for CHARMM. *J Comput Chem* **2008**, *29*, 1859-65.
2. Wu, E. L.; Cheng, X.; Jo, S.; Rui, H.; Song, K. C.; Davila-Contreras, E. M.; Qi, Y. F.; Lee, J. M.; Monje-Galvan, V.; Venable, R. M.; Klauda, J. B.; Im, W., CHARMM-GUI Membrane Builder Toward Realistic Biological Membrane Simulations. *J Comput Chem* **2014**, *35*, 1997-2004.
3. Lee, J.; Cheng, X.; Swails, J. M.; Yeom, M. S.; Eastman, P. K.; Lemkul, J. A.; Wei, S.; Buckner, J.; Jeong, J. C.; Qi, Y. F.; Jo, S.; Pande, V. S.; Case, D. A.; Brooks, C. L.; MacKerell, A. D.; Klauda, J. B.; Im, W., CHARMM-GUI Input Generator for NAMD, GROMACS, AMBER, OpenMM, and CHARMM/OpenMM Simulations Using the CHARMM36 Additive Force Field. *J Chem Theory Comput* **2016**, *12*, 405-413.
4. Jo, S.; Cheng, X.; Lee, J.; Kim, S.; Park, S. J.; Patel, D. S.; Beaven, A. H.; Lee, K. I.; Rui, H.; Park, S.; Lee, H. S.; Roux, B.; MacKerell, A. D.; Klauda, J. B.; Qi, Y. F.; Im, W., CHARMM-GUI 10 years for biomolecular modeling and simulation. *J Comput Chem* **2017**, *38*, 1114-1124.
5. Abraham, M. J.; Murtola, T.; Schulz, R.; Páll, S.; Smith, J. C.; Hess, B.; Lindahl, E., GROMACS: High performance molecular simulations through multi-level parallelism from laptops to supercomputers. *SoftwareX* **2015**, *1–2*, 19-25.
6. Berendsen, H. J. C.; Postma, J. P. M.; Vangunsteren, W. F.; Dinola, A.; Haak, J. R., Molecular-Dynamics with Coupling to an External Bath. *J Chem Phys* **1984**, *81*, 3684-3690.
7. Hess, B.; Bekker, H.; Berendsen, H. J. C.; Fraaije, J. G. E. M., LINCS: A linear constraint solver for molecular simulations. *J Comput Chem* **1997**, *18*, 1463-1472.
8. Hoover, W. G., Canonical Dynamics - Equilibrium Phase-Space Distributions. *Phys Rev A* **1985**, *31*, 1695-1697.
9. Nose, S., A Molecular-Dynamics Method for Simulations in the Canonical Ensemble. *Mol Phys* **1984**, *52*, 255-268.
10. Nose, S.; Klein, M. L., Constant Pressure Molecular-Dynamics for Molecular-Systems. *Mol Phys* **1983**, *50*, 1055-1076.
11. Parrinello, M.; Rahman, A., Polymorphic Transitions in Single-Crystals - a New Molecular-Dynamics Method. *J Appl Phys* **1981**, *52*, 7182-7190.

12. Humphrey, W.; Dalke, A.; Schulten, K., VMD: visual molecular dynamics. *J Mol Graph* **1996**, *14*, 33-8, 27-8.
13. Lindner, B.; Smith, J. C., Sassena - X-ray and neutron scattering calculated from molecular dynamics trajectories using massively parallel computers. *Comput Phys Commun* **2012**, *183*, 1491-1501.
14. Khelashvili, G.; Kollmitzer, B.; Heftberger, P.; Pabst, G.; Harries, D., Calculating the bending modulus for multicomponent lipid membranes in different thermodynamic phases. *Journal of Chemical Theory and Computation* **2013**, *9*, 3866-3871.